Anomalously large negative differential resistance due to Γ-X resonances in type-I GaAs/AlAs superlattices

M. Hosoda, N. Ohtani, K. Tominaga, H. Mimura, and T. Watanabe

ATR Optical and Radio Communications Research Laboratories, Hikaridai, Seika-cho, Soraku-gun, Kyoto 619-02, Japan
(Received 11 November 1996; revised manuscript received 14 May 1997)

An anomalously large negative differential resistance was found in the photocurrent versus reverse bias voltage characteristics (I-V curve) of a type-I GaAs/AlAs superlattice. The scattering and trapping of electrons between Γ states in the GaAs quantum well and X states in the AlAs barrier strongly affect the electron transport, and establish many structures in the I-V curve. [S0163-1829(97)05836-0]

In recent years, functions of the X state have been actively researched mainly for type-II superlattices (SL's).[1] In type-II SL's, photogenerated electrons into the Γ state in a quantum well (QW) rapidly relax down into the X state in a barrier,[1] and stay there until radiative recombination having a long lifetime, e.g., of μs order, occurs with spatial indirect holes in the QW.[2] Conversely, in the case of type-I SL's, it has been believed that electrons staying in the Γ state are quickly swept out to the electrode by an electric field via the Γ states. Although resonances between the Γ and X states have been observed in type-II SL's by Meynadier *et al.*,[3] and although there have been some experimental results on the effect of the X state on carrier transport in SL's or QW systems,[1,4–6] the effect of Γ-X resonances in type-I SL's has not yet been clarified. Very recently, we pointed out that a sufficient influence in carrier transport can be caused by the X state even in type-I SL's.[7–10] To present further information, here we report an interesting phenomenon, i.e., an anomalously large negative differential resistance (NDR) and a high-field domain (HFD) formation which originate Γ-X resonances in a type-I SL. Moreover, various anomalies in photocurrent (Pc) versus reverse bias voltage characteristics (I-V curve) affected by Γ-X resonances were also observed.

A p-i-n diode structure having a nominally undoped SL layer consisting of 100 periods of GaAs/AlAs, with GaAs QW widths of 62 Å and AlAs barrier widths of 34 Å, with 50-nm $Al_{0.4}Ga_{0.6}As$ undoped cladding layers on both SL sides, was grown on a (100)-oriented n^+-type GaAs substrate by molecular-beam epitaxy. Other structures of the p-i-n diode were the same as that described in a previous report.[9] A 632.8-nm HeNe laser irradiated the p-cap side of the sample in a cryostat. The estimated carrier density in the SL region per 1-mW HeNe laser excitation was approximately on the order of 10^{11}/cm^2. All photoluminescence (PL) and I-V curve data were measured at 20 K.

Figure 1 shows the I-V curve of the sample under 1- and 16-mW optical excitation intensity. There are some remarkable things in the figure, i.e., a HFD formation[11,12] from 1 to 5 or 6 V, an anomalously large current dip, and a NDR region around 11 V, some structures in the I-V curve from 15 to 30 V, and a sharp current increase above 30 V. As will be described below, since Γ_1-Γ_2 resonance between adjacent QW's occurs at a higher bias voltage (25 V), the origins of the HFD formation and the NDR should be deduced to other

quantum state resonances. Note that, even under an excitation of only the Γ_1 ground state using a 750-nm cw Ti-sapphire laser, similar experimental results including those described below were observed. This supports the hypothesis that electrons initially in the Γ_1 state, or rapidly relaxed into Γ_1 from Γ_2 under the HeNe laser excitation, cause the phenomena as their carrier transport proceeds.

In general, HFD formations depend on the carrier density in SL's.[12] Figure 2 shows the evolution of the I-V curves of the sample under increasing optical excitation intensities. Note that the transition from normal I-V curves to those having a HFD is strange. Under low excitation, the I-V curves show no waving feature nor anomaly. With increasing excitation intensity, however, the I-V curves begin to show dips (marked B and C) and a peak A. Then, the valley between B and C starts to shrink, and finally, it is packed at around 11 V. Simultaneously, the plateau starting from 2 V expands up to 10 V, and begins to contain a HFD formation that is indicated by the ratchetlike current spikes. The above evolution suggests that an obstruction in carrier transport exists around dips B and C under high carrier densities.

Usually when the carrier transport degrades, the remaining carriers in SL's vanish through a radiative recombination process. As shown in Fig. 3, the shape of the vertically inverted PL intensity curve versus the bias voltage from 0 to 17 V, completely fits the I-V curve. This coincidence was also observed under various photoexcitation intensities greater than 3 μW. This fact supports the assumption that the Γ_1 PL emission, which means Γ_1 occupation, below 17 V is completely dominated by the quality of the carrier transport. In ordinary SL's, the PL emission is quenched by an increase
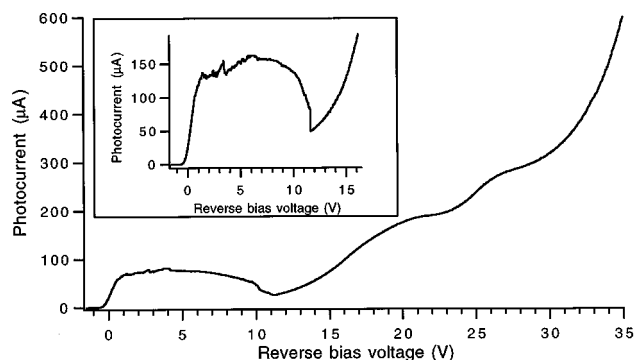
FIG. 1. Photocurrent-voltage characteristics of a sample under 1-mW cw HeNe laser optical excitation at 20 K. Inset: details of a high-field domain formation under 16-mW excitation.
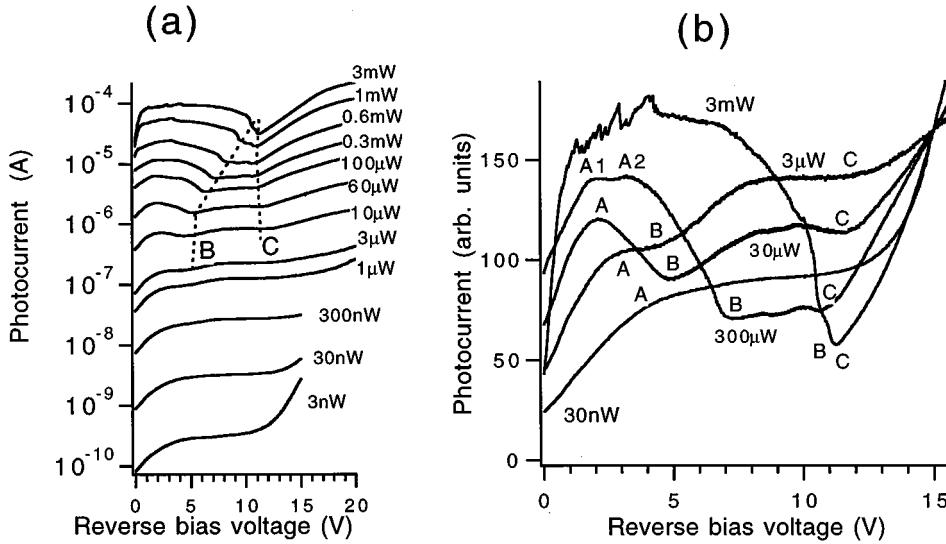
FIG. 2. Photocurrent-voltage characteristics (I-V curve) as a function of the cw HeNe laser excitation intensity at 20 K. In (b), the I-V curves are normalized to the photocurrent value at 15 V for clarity.

in the bias voltage. However in this SL, the PL shows a strong inverse quenching, and shows an even greater PL intensity at 11 V than that under the flatband condition around a -1.5-V forward-bias voltage. This again supports the existence of a strong obstruction for Γ_1 carrier transport at around 11 V, where a large NDR is observed.

To analyze the origin of the phenomenon, a band energy diagram of the SL as shown in Fig. 4 was used. In the calculation, the electron effective mass for GaAs and AlAs is $1.3m_0$ and $1.1m_0$ in the X_z state, and $0.0665m_0$ and $0.1495m_0$ in the Γ state, respectively. A 65% band offset was used to fit the experimental data. We assumed a 100-nm expansion of the intrinsic layer due to the depletion of the p-i-n diode. We neglected higher subband states and state crossings, where the existence of carriers is not expected under our experimental condition. The calculated Γ_1 energies of the electron agreed well with the measured energies from Pc spectra (not shown). It should be noted that the X state treated in our present work resulted from the quantization of the X valley along the growth direction [001], i.e., the so-called X_z state which often couples with the Γ state.

Because the probability density of the wave function, which leaks through remote barriers, becomes small in the barrier width (34 Å), we consider only the first-nearest-neighbor couplings for Γ_n states. However, we apply the

second-nearest-neighbor couplings for the Γ_1-X_n resonances. This is because, as shown in the schematic energy-band diagram in Fig. 4, when an electron tunnels through one barrier and relaxes down to the next Γ_1 state, an X_n state in the neighboring barrier having a strong scattering cross section[1,7] is thought to be able to still catch the electron. The above tunneling capability of one barrier has been confirmed by PL from Γ_1-Γ_2 resonance in this sample.[9] From Fig. 4, there exist several subband crossings between adjacent layers as shown in Table I. The notations in the table assume carrier transport from the left state to the right state, because the latter state has a lower-energy level than the former under the electric field.

We disregarded the contribution of holes to the phenom-

FIG. 3. Photocurrent and photoluminescence (PL) intensity of a Γ_1-hh$_1$ ground-state transition as a function of the reverse bias voltage under 3-mW cw HeNe laser excitation at 20 K. The PL intensity is inverted, i.e., upset vertically, to allow a comparison of the shapes of both curves.
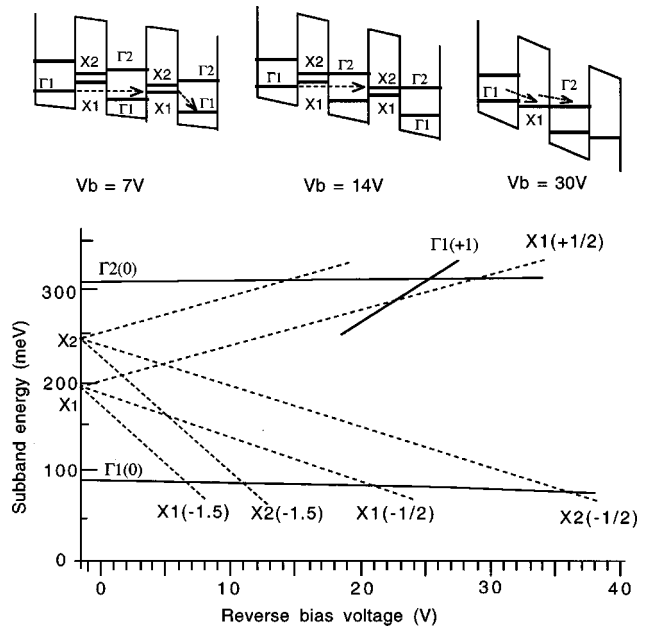
FIG. 4. Energy fan charts of calculated subbands of the sample as a function of the reverse bias voltage, and the schematic band diagram. Energy zero means the conduction-band energy of bulk GaAs. The numbers in parentheses indicate the distance in units of superlattice period from a particular quantum well indexed by 0. For example, $\Gamma_2(1)$ means a Γ_2 eigenstate belonging to the first neighboring wells.

TABLE I. Calculated resonance voltages.

State resonance	Bias voltage (V)
$X_1(+0.5)-X_2(-0.5)$	5
$\Gamma_1(0)-X_1(-1.5)$	7
$\Gamma_1(0)-X_2(-1.5)$	11
$X_2(+0.5)-\Gamma_2(0)$	14
$\Gamma_1(0)-X_1(-0.5)$	21
$\Gamma_1(+1)-\Gamma_2(0)$	25
$X_1(+0.5)-\Gamma_2(0)$	30
$\Gamma_1(0)-X_2(-0.5)$	36

ena in this paper owing to the following reasons. First, similar phenomena were also observed under 488-nm Ar laser excitation. Because the penetration depth of the 488-nm light is very short from the p cap, e.g., less than 100 nm from the top surface, holes are swept out quickly toward the p cap almost without running through the SL; thus electrons dominate the carrier transport in the SL. Second, resonance voltages among the hole states cannot solve the phenomena. The voltages are 2.5 V for hh$_1$-lh$_1$, 5 V for hh$_1$-hh$_2$, 9 V for hh$_2$-hh$_3$, and 17 V for hh$_1$-hh$_3$. Because all of these resonances promote the carrier transport, they cannot solve the strong obstruction in carrier transport shown in Figs. 1–3. Moreover, it is known that the HFD formation splits the PL spectra as previously reported for the electron state resonances.[13] If the HFD formation originated from the hole resonances, another PL emission from a higher-energy transition, e.g., Γ_1-lh$_1$ PL, would be observed. However, we have not observed any such PL during the HFD formation. Although we observed a PL component at a corresponding wavelength of the Γ_1-lh$_1$ transition, no correlation was found between the PL intensity and the hole state resonances. If the domain formation originated from the Γ_1 and X states, no PL peak from the X states would be observed, and, therefore, this interpretation is more plausible than that from the hole resonances. Third, in general, holes hardly move due to their heavy effective mass,[14] and scarcely contribute photocurrent.[15] Holes may contribute current voltage characteristics only when other resonances of the electron states do not exist.[16] However, when the drift speed of the electron is faster than the hole, the nonuniform electric field caused by the hole space charges will be masked by the electron movement. In this case, the hole space charges will merely screen the entire electric field in the SL uniformly. Although some of the phenomena at lower voltages might be explained by the hole resonances, from the above consideration we explain the phenomena in this paper by electron state resonances.

To confirm the energy levels of the states in Fig. 4, we observed a PL emission from a higher Γ_2 subband resonating with lower-energy states. When the X_1 states resonate with the Γ_2 state, trapped carriers in the X_1 state can escape to the Γ_2 state, and can emit PL due to the Γ-X mixing.[9] The sample in this paper is one of the same samples in Ref. 9. Clear PL emissions from $\Gamma_1(+1)-\Gamma_2(0)$ and $X_1(+1/2)-\Gamma_2(0)$ resonances were observed,[9] and both PL intensities were almost on the same order. The resonance voltages of the PL agree well with those in Table I, and support the validity of our calculation shown in Fig. 4.

Because the oscillator strength of the X_1 recombination with holes in QW's is very weak due to spatial and momentum indirect transitions, the PL emission from the above $X_1(+1/2)-\Gamma_2(0)$ resonance supports the assumption that a certain amount of carriers exist in the X_1 state. This means that a strong Γ-X scattering exists in type-I SL's, and indicates a trapping capability of the carriers into the X_n, i.e., obstruction in carrier transport.[10] When an X_n state energy position in an adjacent barrier comes close to, or goes lower than, that of the Γ_1 state under an electric field, carriers will be trapped into the X_n state. Since the nonresonant X-Γ transfer, that is, the escape process from the trap, is considerably slower than the Γ-X transfer due to a difference of the density of state between both states,[17] trapped carriers cannot easily escape from the X_n traps. In contrast to the above, when the Γ_2 state in the adjacent QW goes below the X_n state, carriers are able to escape through the X_n-Γ_2 transfer path.[7,8] In this case, the current output increases.

Considering all of this, Γ-X transfers corresponding to $\Gamma_1-X_1(-1.5)$ at about 7 V and $\Gamma_1-X_2(-1.5)$ at 11 V (cf. Fig. 4 and Table I) reduce the carrier transport. Because the overlap integral of Γ_1-X_2 is greater than that of Γ_1-X_1 from the symmetry of the wave functions, Γ_1-X_2 at 11 V can capture the electron efficiently. Furthermore, trapped electrons into X_2 will relax down into X_1, not Γ_1, because they have the same momentum and density of state. This will degrade the carrier transport even more. The large dip in the I-V curve around 11 V, i.e., the rapid decrease in current, corresponds to the above Γ_1-X_2 resonance. A similar degradation in the carrier transport is also observed around 22 V in Fig. 1 due to the $\Gamma_1-X_1(-0.5)$ resonance.

After the above Γ_1-X_2 resonance voltage at 11 V, when the $X_2(+0.5)-\Gamma_2(0)$ transfer properly operates, the carrier transport will be promoted through the $X_2-\Gamma_2-X_2$ path. The current increase in the I-V curve from 12 V reflects this circumstance. A similar condition is found above 30 V caused by the $X_1(+0.5)-\Gamma_2(0)$ transfer,[9,10] and the current increases rapidly, as shown in Fig. 1. Another increase in the current above 25 V can be easily identified as the $\Gamma_1-\Gamma_2$ resonance. Although there is a $\Gamma_1(0)-X_2(-0.5)$ resonance at 36 V, this resonance does not display its trapping ability, because carriers that relax down into the X_1 state from X_2 are rapidly swept out via the $X_1-\Gamma_2$ path. Therefore, the carrier transport sharply increased above 30 V and an avalanche breakdown was observed at 37 V.

The next feature to be analyzed is HFD formation below 10 V. At lower voltages, there are two resonance voltages having an efficient carrier sweep-out rate; they are $\Gamma_1-\Gamma_1$ LO-phonon-assisted tunneling near 1 V, and X_1-X_2 resonant tunneling around 5 V. These voltages agree well with the starting and end voltages of the HFD formation region in the I-V curve.[12] However, carrier occupation in the X_1 state is improbable, because $\Gamma_1(0)-X_1(-1.5)$ scattering cannot occur until 7 V. We solved this discrepancy with the following hypothesis: After a higher-energy level in the Γ_1 state is filled with a high density of carriers caused by a degraded carrier transport, Γ_1-X_1 scattering is probable below 7 V because of a filling to a higher Γ_1 state energy and because of increased carrier scattering into a higher X_1 state between thermalized hot carriers or by assistance of the LO

phonon.[18–21] Therefore, we identified the HFD formation by $\Gamma_1-\Gamma_1$ tunneling in a low-field domain (LFD), and X_1-X_2 resonant tunneling in a HFD.[5]

The last remaining feature is the evolution of the *I-V* curve shown in Fig. 2. In general, the shape of an *I-V* curve as a function of the excitation intensity is thought to be affected by two factors: electric-field screening due to space-charge buildup, and changes in the carrier scattering or relaxation rate due to state filling. However, the occupation density of the state is dominated by the carrier transport, which is also a function of the above factors. Therefore, the relation is nonlinear for the excitation. We thought that the key point is for the carrier density to flow in each transport path, e.g., $\Gamma_1-\Gamma_1$, X_1-X_2, etc. Assuming that each carrier transport path has a limiting capacity to allow the flow of carriers, or has a limit as to the number of carriers that can pass in a unit time, i.e., the inverse value of the transfer time through the path, the current under a high carrier density will saturate. Then a dip will appear in the *I-V* curve with an increase in excitation, and the stopped carriers exceeding the flow capacity will establish an electric field screening that will change the inner electric field in the SL, i.e., a sort of electric-field domain formation will be established.

The flow capacities of each carrier path should each have a different nonlinearity as a function of the carrier density, and the *I-V* characteristics should be modulated by the carrier densities. The evolution of the *I-V* curve in Fig. 2 is thought to show the above relation. As shown in Fig. 2, current peak A corresponding to nonresonant $\Gamma_1-\Gamma_1$ tunneling moves toward a lower voltage as the excitation carrier density is increased. Simultaneously, current dip B, which is thought to correspond to increasing Γ_1-X_1 scattering, moves toward the higher voltage side. Therefore, when the bias voltage is in the region between A and B, a HFD region and a LFD region may be established in the SL, since the current dip B stops the carriers and generates space charges. As shown in Fig. 2, at 300-μW excitation, two branches, $A1$ and $A2$, arise between A and B. This implies the start of the separation of LFD by $\Gamma_1-\Gamma_1$ and HFD by X_1-X_2. Then, as the carrier density is further increased, these two branches grow to an ordinary electric field domain which leads to ratchetlike current spikes. The number of observed current spikes of about 100, which coincides with the number of the SL period, supports the assumption that a HFD formation is fairly well established and the domain boundary moves every SL period with an increase in the bias voltage.[12] Simultaneously, the right-side slope of branch $A2$ expands toward a higher voltage. This is thought to arise from the increasing carrier transport originating from X_1-X_2 nonresonant tunneling under high carrier densities. This evolution implies that the tunneling between X states is promoted greatly as state filling in the X states grows.

Note that the position of current dip C does not move so much. This means that the obstruction process caused by Γ_1-X_2 scattering has a strong efficiency even when the carrier density is high. Even when the carrier transport may be dominated by the above X_1-X_2 transfer path, once the X_2 state is filled by the Γ_1-X_2 scattering at point C, it is considered that the carriers in the X_1 state cannot enter into the X_2 state. This will inhibit the X_1-X_2 tunneling and cause a large dip, i.e., NDR, in the *I-V* curve, as shown by the *I-V* curves under high excitation above 3 mW in Figs. 1 and 2.

In conclusion, we have observed an anomalously large NDR and a HFD formation in a type-I SL. These phenomena were explained as a result of carrier transport among Γ and X states.

[1] J. Feldmann and E. O. Göbel, in *Optics of Semiconductor Nanostructures*, edited by F. Henneberger, S. Schmitt-Rink, and E. O. Göbel (Akademie Verlag, Berlin, 1993), Chap. I. 7, and references therein.

[2] M. Nakayama, K. Imazawa, K. Suyama, I. Tanaka, and H. Nishimura, Phys. Rev. B **49**, 13 564 (1994).

[3] M. H. Meynadier, R. E. Nahory, J. M. Worlock, M. C. Tamargo, J. L. de Miguel, and M. D. Sturge, Phys. Rev. Lett. **60**, 1338 (1988).

[4] E. E. Mendez, E. Calleja, C. E. T. Gonçalves da Silva, L. L. Chang, and W. I. Wang, Phys. Rev. B **42**, 5809 (1990).

[5] Y. Zhang, X. Yang, W. Liu, P. Zhang, and D. Jiang, Appl. Phys. Lett. **65**, 1148 (1994).

[6] A. Sibille, J. F. Palmier, H. Wang, and R. Planel, Appl. Phys. Lett. **65**, 2179 (1994).

[7] M. Hosoda, N. Ohtani, H. Mimura, K. Tominaga, P. Davis, T. Watanabe, G. Tanaka, and K. Fujiwara, Phys. Rev. Lett. **75**, 4500 (1995).

[8] H. Mimura, N. Ohtani, M. Hosoda, K. Tominaga, T. Watanabe, G. Tanaka, and K. Fujiwara, Appl. Phys. Lett. **67**, 3292 (1995).

[9] M. Hosoda, H. Mimura, N. Ohtani, K. Tominaga, K. Fujita, T. Watanabe, H. Inomata, and M. Nakayama, Phys. Rev. B **55**, 13 689 (1997).

[10] M. Hosoda, K. Tominaga, N. Ohtani, H. Mimura, and M. Nakayama, Appl. Phys. Lett. **70**, 1581 (1997).

[11] L. Esaki and L. L. Chang, Phys. Rev. Lett. **33**, 495 (1974).

[12] H. T. Grahn, in *Semiconductor Superlattices*, edited by H. T. Grahn (World Scientific, Singapore, 1995), Chap. 5, and references therein.

[13] H. T. Grahn, H. Schneider, and K. v. Klitzing, Appl. Phys. Lett. **54**, 1757 (1989).

[14] F. Capasso, K. Mohammed, A. Y. Cho, R. Hull, and A. L. Hutchinson, Phys. Rev. Lett. **55**, 1152 (1985).

[15] F. Agulló-Rueda, H. T. Grahn, A. Fischer, and K. Ploog, Phys. Rev. B **45**, 8818 (1992).

[16] H. Schneider, H. T. Grahn, K. von Klitzing, and K. Ploog, Phys. Rev. B **40**, 10 040 (1989).

[17] J. Feldmann, M. Preis, E. O. Göbel, P. Dawson, C. T. Foxon, and I. Galbraith, Solid State Commun. **83**, 245 (1992).

[18] P. W. M. Blom, C. Smit, J. E. M. Haverkort, and J. H. Wolter, Appl. Phys. Lett. **62**, 2393 (1993).

[19] F. Agulló-Rueda, H. T. Grahn, and K. Ploog, Phys. Rev. B **49**, 14 456 (1994).

[20] O. E. Raichev, Phys. Rev. B **49**, 5448 (1994).

[21] B. Deveaud, F. Clérot, A. Regreny, R. Planel, and J. M. Gérard, Phys. Rev. B **49**, 13 560 (1994).